Supporting Information for "Broad consistency between observed and simulated trends in sea surface temperature patterns"

Dirk Olonscheck[1], Maria Rugenstein[1], Jochem Marotzke[1]

[1]Max Planck Institute for Meteorology, Bundesstrasse 53, 20146 Hamburg, Germany

Contents of this file

March 20, 2020, 11:18am

Table S1. Minimum, average, and maximum Pearson correlation coefficient, r, of the annual global mean SST evolution between the realizations of each model ensemble and the averages across observational estimates. A small spread and a high value of r indicate that the ensemble members resemble the observed SST evolution, while a high spread and a low value of r indicate less agreement. Compare with Figure 1.

Model ensemble	r_{min}	r_{avg}	r_{max}
CMIP5	0.38	0.72	0.84
CMIP6	0.48	0.76	0.88
CanESM2	0.77	0.83	0.88
CESM-LE	0.58	0.69	0.81
CSIRO-Mk3-6-0	0.37	0.54	0.64
GFDL-ESM2M	0.66	0.78	0.86
IPSL-CM6A-LR	0.70	0.78	0.86
MIROC6	0.54	0.65	0.73
MPI-GE	0.68	0.74	0.82

Table S2. Percent of ensemble members of each model with a globally averaged SST trend larger than the observed COBE-SST2 trend for the four trend periods. In the early warming period, no single realization captures the observed warming, whereas in the recent warming period, the representation of the observed warming strongly differs between the models. For the recent hiatus, all models warm more than observed.

Model ensemble	1915-1944	1945-1974	1975-2004	1995-2014
CMIP5	0	90	0	-
CMIP6	0	41	39	96
CanESM2	-	-	94	100
CESM-LE	-	39	2	-
CSIRO-Mk3-6-0	0	3	13	96
GFDL-ESM2M	-	-	26	93
IPSL-CM6A-LR	0	67	54	96
MIROC6	0	34	2	90
MPI-GE	0	79	24	-
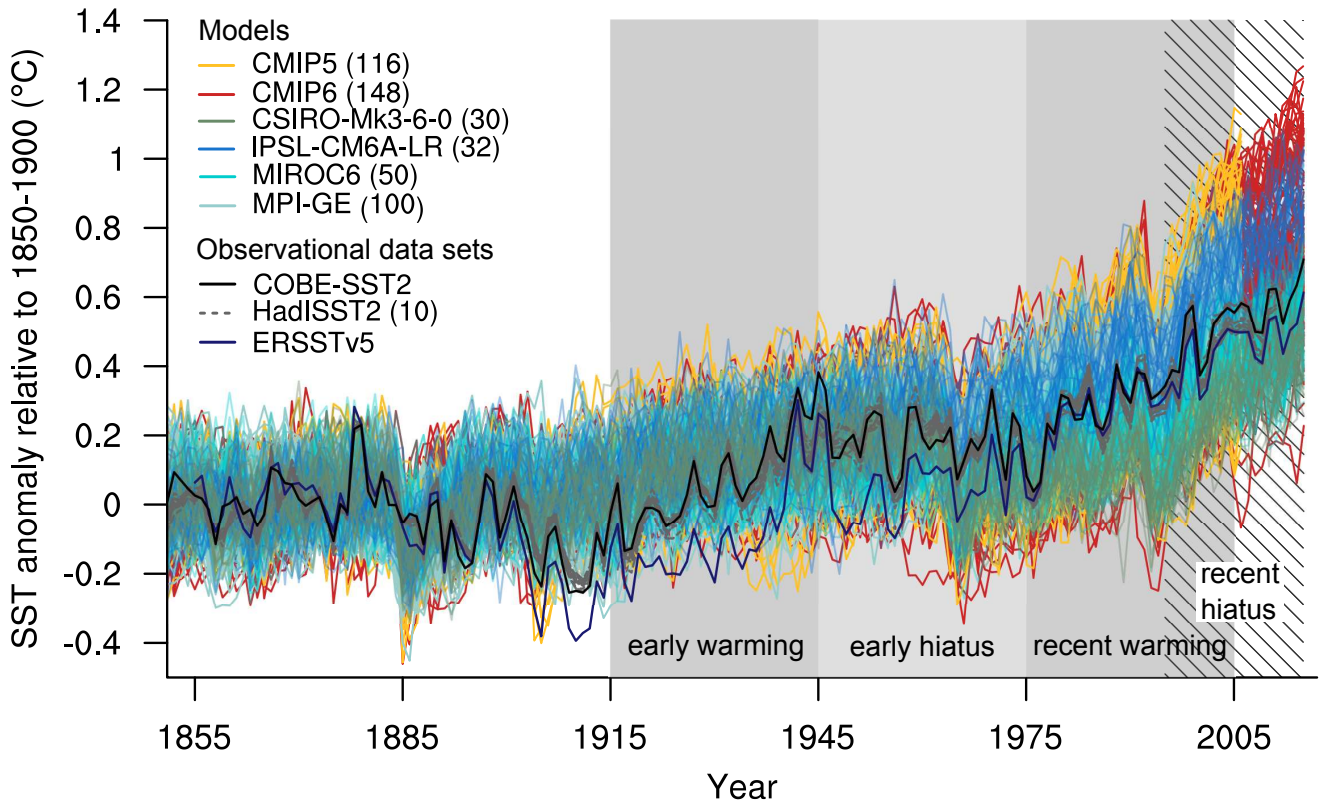
Figure S1. Same as Figure 1, but with respect to the reference period 1850-1900. Note that only the single-model large ensembles are shown with simulations that start in 1850.
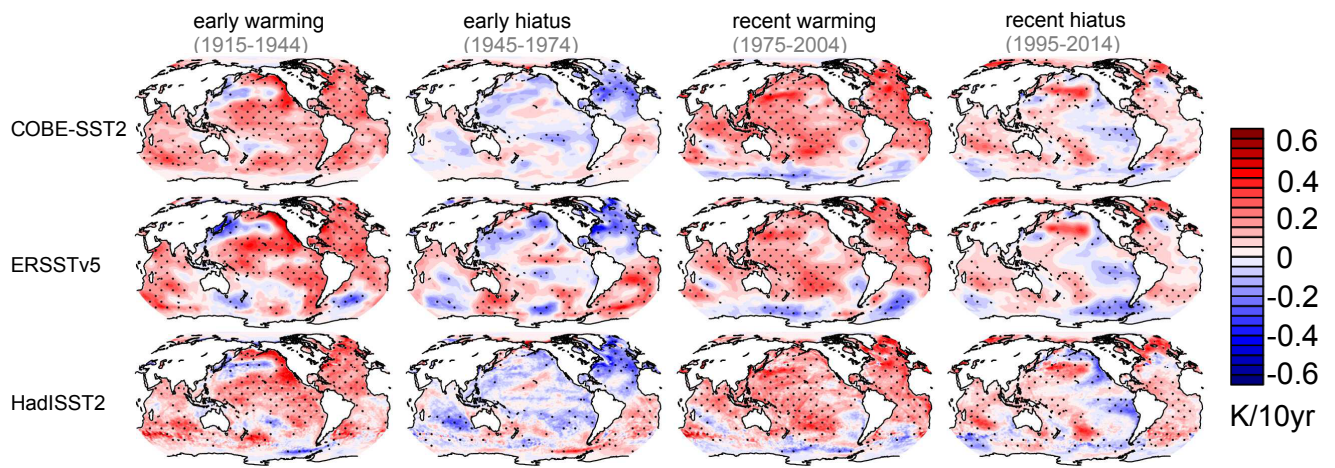
Figure S2. Trend in SST patterns in the three observational data sets COBE-SST2, ERSSTv5, and HadISST2 for the four characteristic trend periods. Stippling marks statistically significant trends at the 95% level. Note that the observational uncertainty is much greater than the difference between the data sets (Kennedy, 2014).

recent warming
(1975-2004)

recent hiatus
(1995-2014)

COBE-SST2

CanESM2

#18   0.6

#1   0.49

CESM-LE

#38   0.31

CSIRO-Mk3-6-0

#3   0.41

#3   0.31

K/10yr

GFDL-ESM2M

#28   0.57

#3   0.35

0.6
0.4
0.2
0
-0.2
-0.4
-0.6

IPSL-CM6A-LR

#24   0.58

#20   0.35

MIROC6

#42   0.5

#47   0.48

MPI-GE

#62   0.48

CMIP6

0.6

0.49

CMIP5

0.61
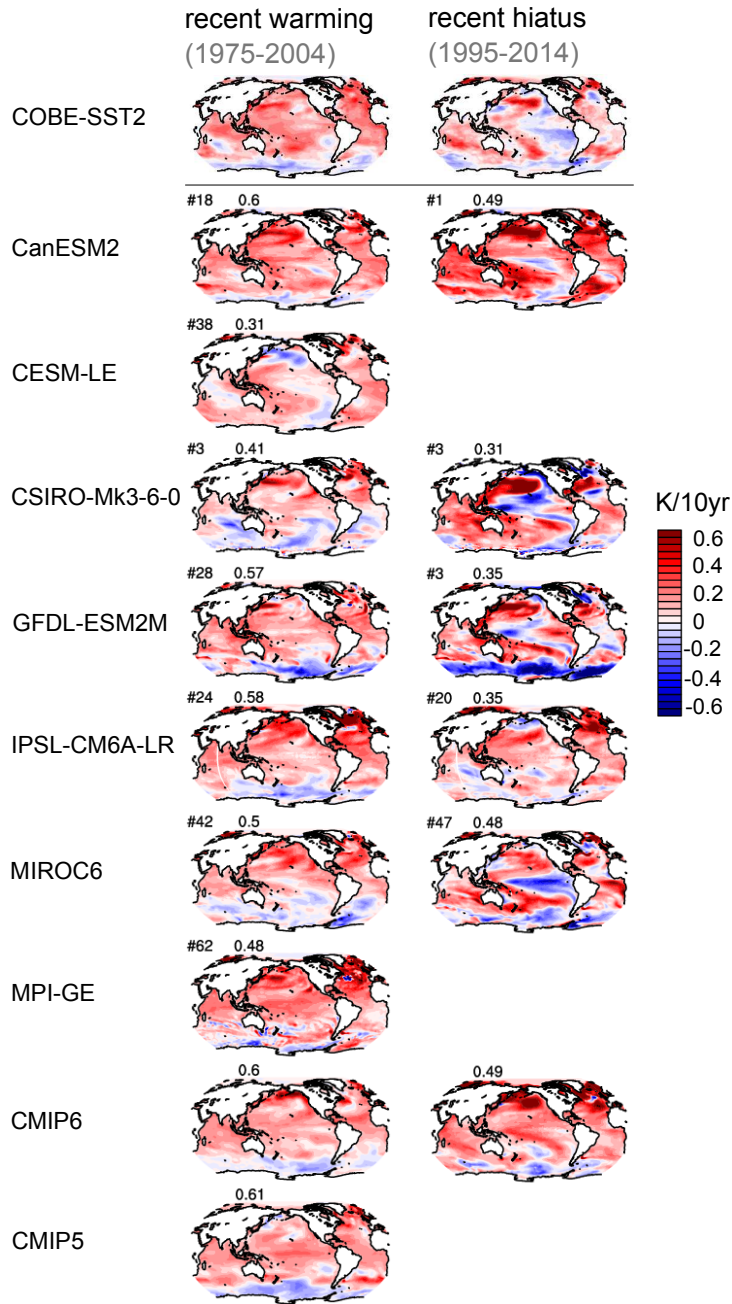
Figure S3.   COBE-SST2 trend pattern and model simulations with the highest pattern correlation with COBE-SST2 for the period 1975-2004 (left column) and the period 1995-2014 (right column). The numbers on top of each panel specify the number of the ensemble member, and the value of r, respectively.
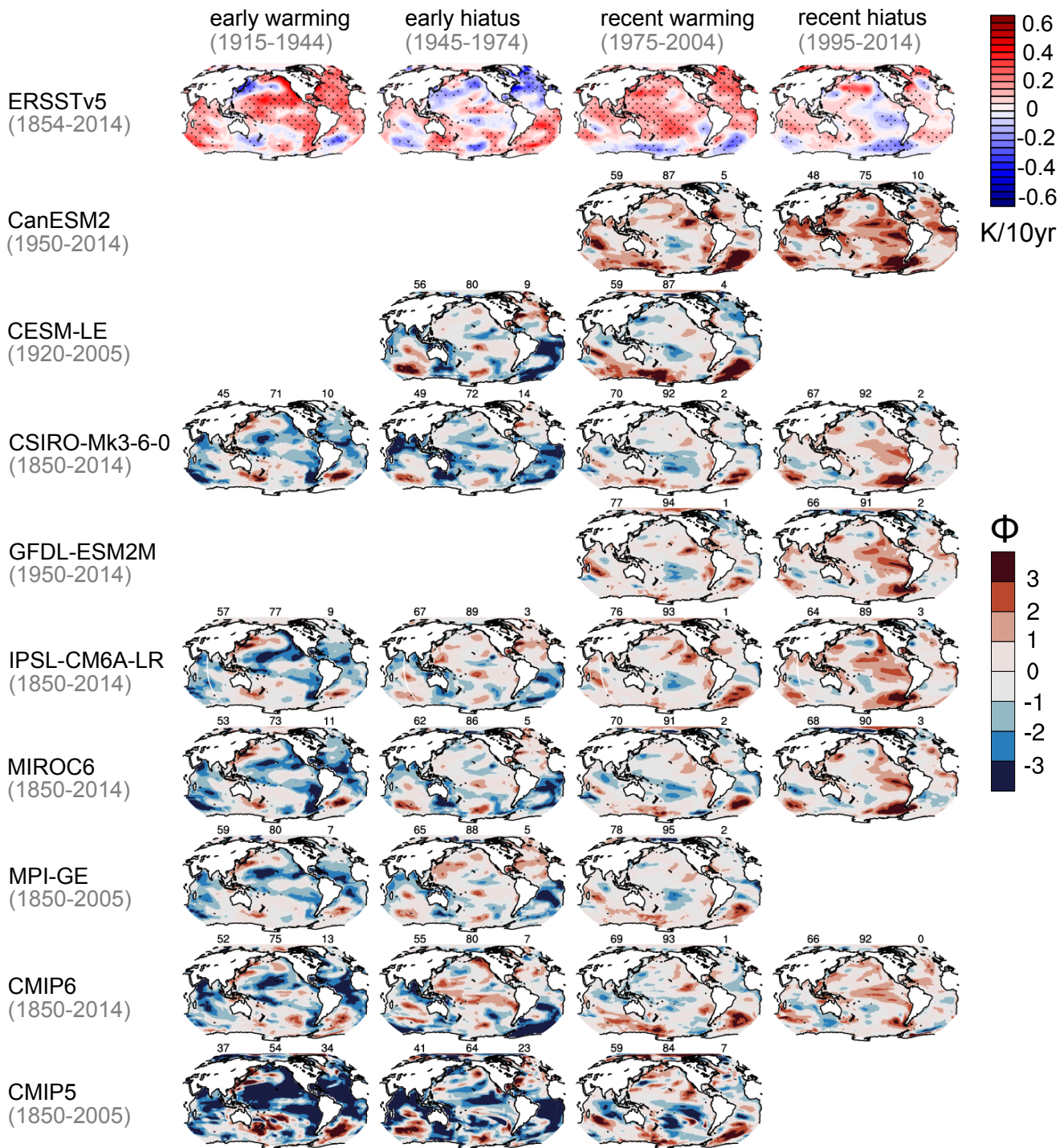
Figure S4. Same as Fig. 2, but using the observational data set ERSSTv5.
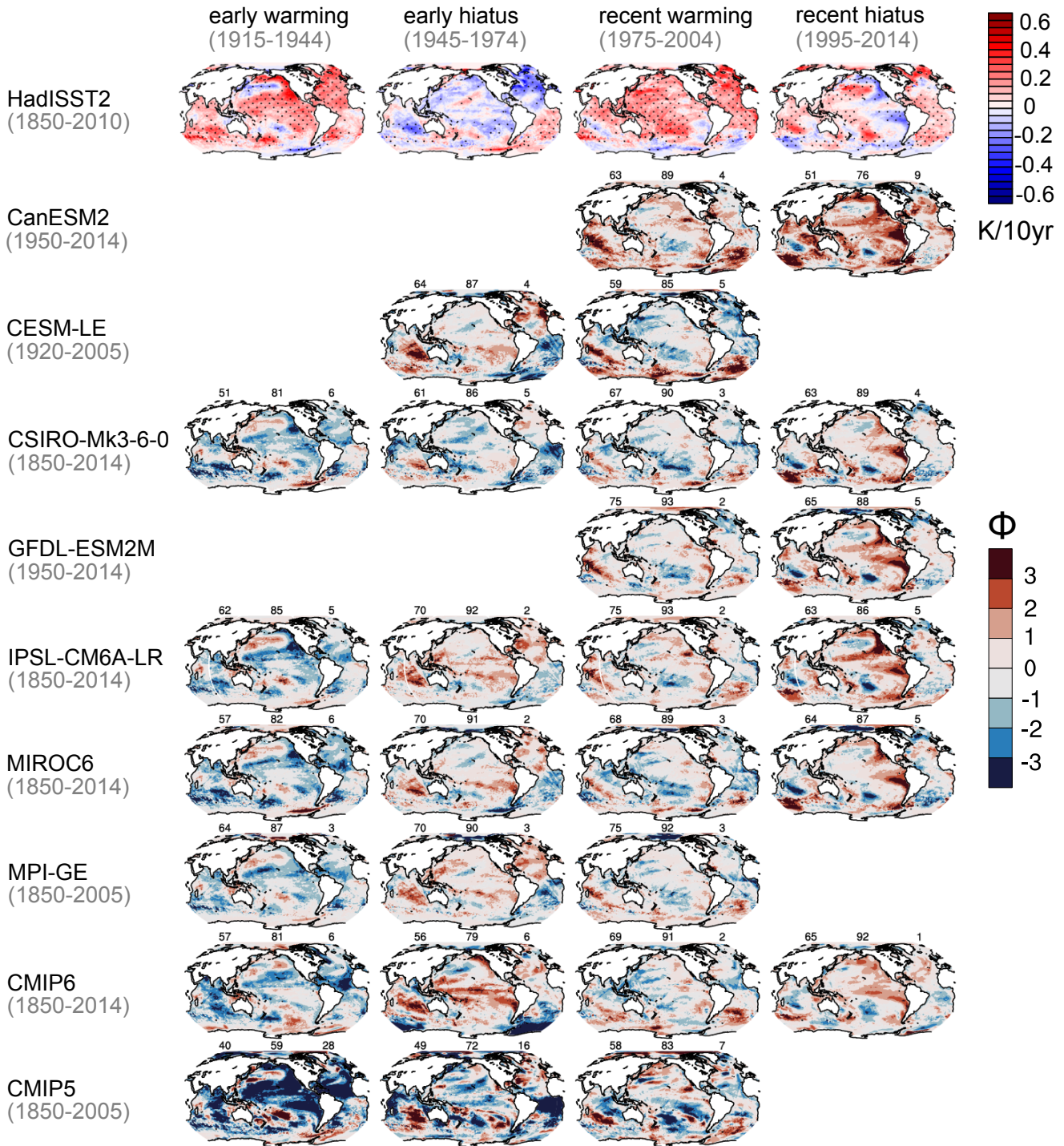
Figure S5. Same as Fig. 2, but using the observational data set HadISST2.
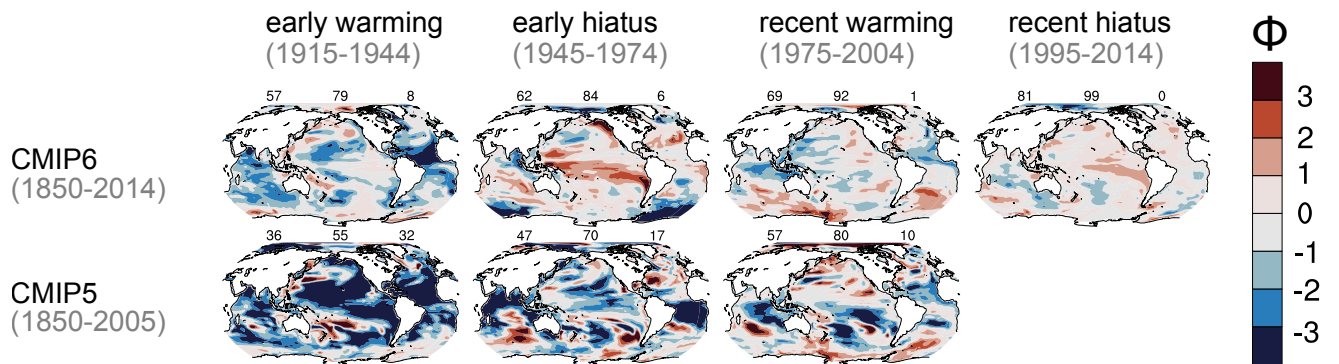
Figure S6. Same as Fig. 2 for CMIP5 and CMIP6, but for all simulations in CMIP5 and CMIP6, including all ensemble members for each model instead of just the first ensemble member of each model as shown in Fig. 2 in the main text.
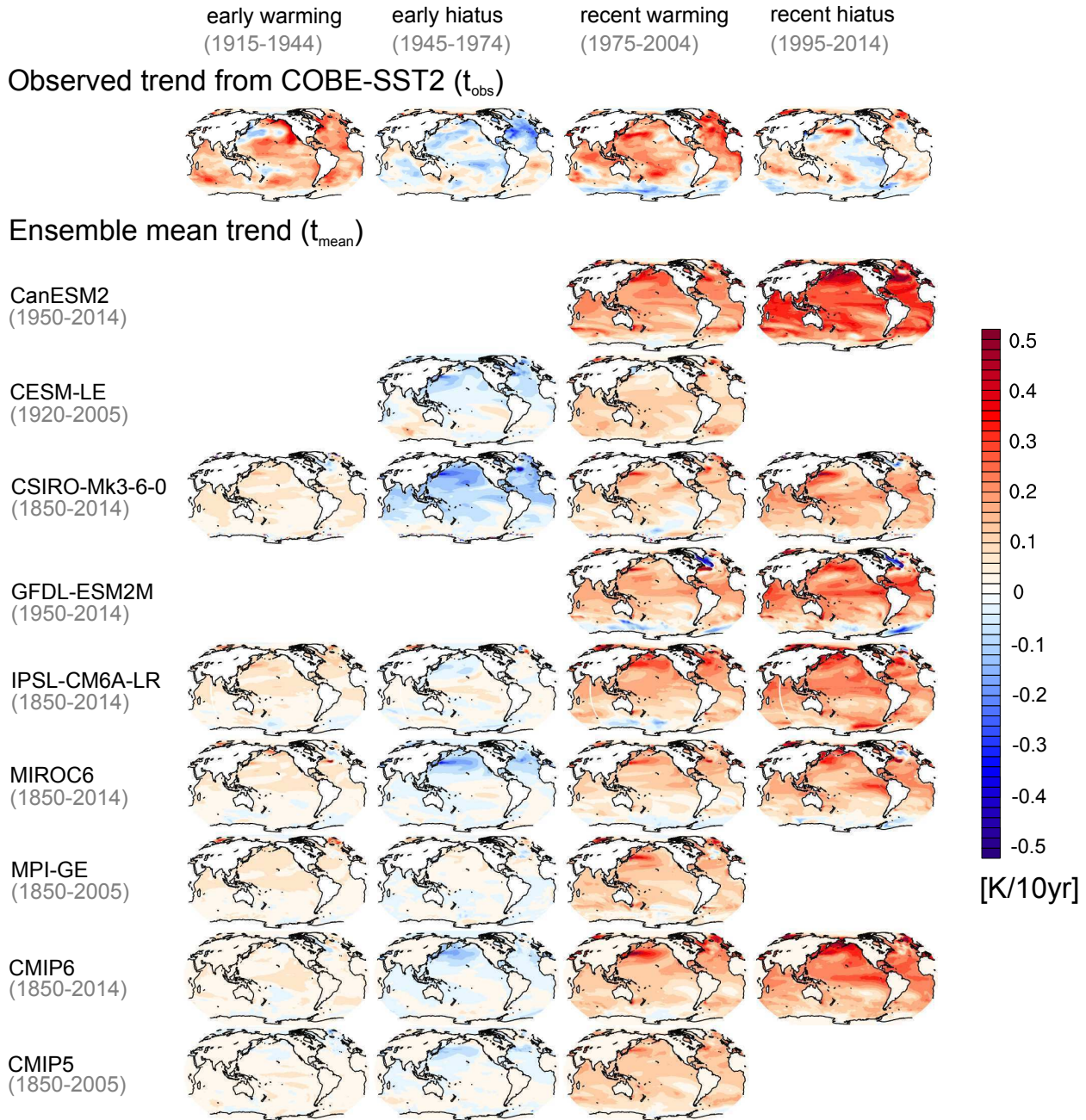
Figure S7. Terms of Equation 1 for all model ensembles. The observed COBE-SST2 trend (top row), and the ensemble mean trend of each model ensemble (other rows) for the four characteristic historical periods. The ensemble standard deviation σ of all model ensembles is shown in Figure S8.
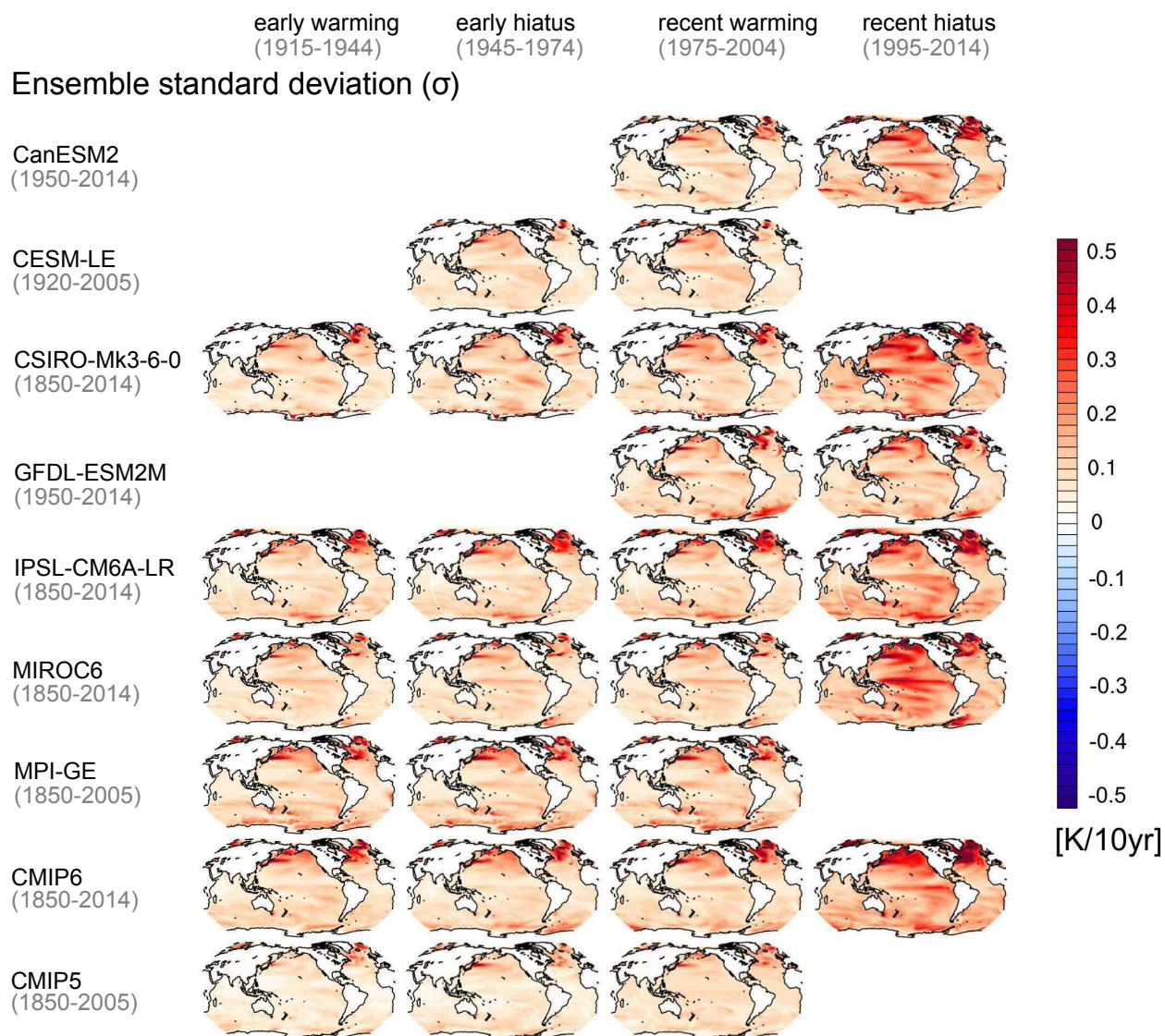
Figure S8. **(As Figure S7, continued)** The ensemble standard deviation σ of all model ensembles for the four characteristic historical periods. Note that the larger ensemble standard deviation in the last column is caused by the computation over only a 20-year period.